

Photolysis of FeOH^{2+} and FeCl^{2+} in Aqueous Solution. Photodissociation Kinetics and Quantum Yields

Victor A. Nadtochenko^{*,†} and John Kiwi^{*}

Institute of Physical Chemistry II, Swiss Federal Institute of Technology (EPFL),
Lausanne 1015, Switzerland

Received April 24, 1998

Photodissociation of FeOH^{2+} and FeCl^{2+} complexes has been studied by pulsed laser spectroscopy ($\lambda = 347$ nm) techniques. Transient bleaching of FeOH^{2+} was observed due to the dissociation $\text{FeOH}^+ \rightarrow \text{Fe}^{2+} + \text{OH}^\bullet$ (at $\lambda = 347$ nm). The observed bleaching involved the photoreduction of the species FeOH^{2+} to iron(II) complexes. These latter species showed a much lower absorption. Concomitant formation of the $\text{Cl}_2^{\bullet-}$ anion radical was observed due to the reactions $\text{FeCl}^{2+} \rightarrow \text{Fe}^{2+} + \text{Cl}^\bullet$ (at $\lambda = 347$ nm) and $\text{Cl}^\bullet + \text{Cl}^- \rightarrow \text{Cl}_2^{\bullet-}$. The experimental findings allowed us to suggest a reaction sequence involving Cl^\bullet , $\text{Cl}_2^{\bullet-}$, $\text{ClOH}^{\bullet-}$ and OH^\bullet radicals. The quantum yields found by laser kinetic spectroscopy for FeOH^{2+} and FeCl^{2+} photodissociation were 0.21 ± 0.04 and 0.5 ± 0.1 , respectively.

Introduction

Iron(III) ions in aqueous solution are known to form complexes of the type $\text{Fe}^\bullet\text{X}^{2+}$ ($\text{X} = \text{Cl}^-, \text{Br}^-, \text{OH}^-, \text{NCS}^-$).^{1–3} Iron(III) ions with weak anionic ligands such as NO_3^- and ClO_4^- hydrolyze in aqueous solution, forming the FeOH^{2+} and hydroxy type complexes.³ In the presence of the Cl^- anionic ligand, FeOH^{2+} and FeCl^{2+} coexist.^{4,5} The equilibria of the Fe^{3+} ion with OH^- and Cl^- in aqueous solutions have been investigated during the past few decades and are reported in the literature.^{3–6} Recently, the photolysis of iron(III) species was seen to accelerate the formation of carboxylic acids and the oxidation of SO_2 in atmospheric droplets.^{7–9} The oxidation of organic compounds was reported to occur due to photochemically induced OH^\bullet radicals in aqueous media.¹⁰ Photolyses of FeOH^{2+} complexes have also been suggested to account for the photoassisted Fenton catalysis,^{11–14} and the photochemistry of FeOH^{2+} and FeCl^{2+} complexes has been shown to be important during Fe^{2+} – Fe^{3+} recycling in marine waters.⁵ Knowledge about the quantum yield of photodissociation of FeOH^{2+} and FeCl^{2+} is important for model calculations of processes taking place in natural waters.^{11–15}

The reported quantum yields of photodissociation of FeOH^{2+} and FeCl^{2+} are based on steady-state photolysis using organic compounds or iron(II) as radical scavengers.^{1,2,7,23} A large measure of uncertainty was introduced into these measurements due to the occurrence of secondary radical reactions. For instance, the photodissociation $\text{FeCl}^{2+} \rightarrow \text{Fe}^{2+} + \text{Cl}^\bullet$ was suggested in 1949.^{16–18} Low quantum yield for this reaction has been determined by using methyl methacrylate^{19–22} or a benzoic acid^{19,20} as a scavenger, whereas the quantum yield of this reaction has been reported to be 9.3% by using *tert*-butyl alcohol.²³

The present study is designed (a) to establish the mechanism of the primary photochemical steps during the photolysis of (FeOH^{2+}) and (FeCl^{2+}) complexes and (b) to determine the quantum yield of photodissociation of these compounds. Nanosecond laser photolysis has been selected as an appropriate experimental technique. The iron(III) concentrations used (< 1 mM) are close to the iron(III) concentrations existing in clouds and fog droplets, where iron is found in the range 10^{-4} – 10^{-1} mM.⁷ At iron(III) concentrations < 1 mM and pH between 0.5 and 3.0 the formation of dimers and polynuclear iron complexes is less important and the composition of the iron(III) complex is well-defined.^{3–6} These reactions reported in this study play a central role during degradation of organic contaminants in water systems when $\bullet\text{OH}$ radicals and Cl^- species are in solution.^{11–14}

Experimental Section

Materials and Samples. $\text{FeCl}_3 \cdot 6\text{H}_2\text{O}$, $\text{Fe}(\text{ClO}_4)_3 \cdot 9\text{H}_2\text{O}$, NaClO_4 , NaCl , and anthracene were Fluka p.a. grade and were used as received. The solution pH was adjusted with HClO_4 or HCl . The acid

[†] On a leave of absence from the Institute of Chemical Physics in Chernogolovka of RAS, Chernogolovka, Moscow district 142432, Russia.

- (1) Balzani, V.; Carassiti V. In *Photochemistry of Coordination Compounds*; Academic Press: London, 1970; p 145.
- (2) Horvath, O.; Stevenson, K. *Charge-Transfer Photochemistry of Coordination Compounds*; VCH: Weinheim, Germany, 1993; p 218.
- (3) Rabinowitch, E.; Stockmayer, W. *J. Am. Chem. Soc.* **1942**, *64*, 335.
- (4) Byrne, R.; Kester, D. *J. Solution Chem.* **1978**, *7*, 373.
- (5) Byrne, R.; Kester, D. *J. Solution Chem.* **1981**, *10*, 51.
- (6) Knight, R. Sylva, R. *J. Inorg. Nucl. Chem.* **1975**, *37*, 779.
- (7) Faust, C.; Hoigné, J. *J. Atmos. Environ.* **1990**, *24*, 79, 1990.
- (8) Graedel, T. E.; Wescher, C. J.; Mandich, M. L. *Nature* **1985**, *317*, 240.
- (9) Faust, B. C., Hoffmann, M. R. *Environ. Sci. Technol.* **1986**, *20*, 943.
- (10) Baxendale, J. H.; Magee, J. *Trans. Faraday Soc.* **1955**, *51*, 205.
- (11) Ruppert, G.; Bauer, G.; Heisler, G. *J. Photochem. Photobiol. A.* **1993**, *73*, 75.J.
- (12) Prousek, J. *Chem. Listy*, **1995**, *89*, 11.
- (13) Lipchynska-Kochany, E. *Environ. Sci. Technol.* **1992**, *26*, 313.
- (14) Pignatello, J. *J. Environ. Sci. Technol.* **1992**, *26*, 313.
- (15) King, D. W.; Charnecki, S. E. *Marine Chem.* **1993**, *44*, 105.

- (16) Evans, M. G.; Uri, N. *Nature* **1949**, *164*, 404.
- (17) Evans, M. G.; Santappa, M.; Uri, N. *J. Polym. Sci.* **1951**, *7*, 243.
- (18) Bates, H. G. C.; Uri, N. *J. Am. Chem. Soc.* **1953**, *75*, 2754.
- (19) David, F.; David, P. G. *J. Phys. Chem.* **1976**, *80*, 579.
- (20) David, P. G. *J. Chem. Soc., Chem. Commun.* **1972**, 1294.
- (21) Palit, S.R.; Saha, M. K. *J. Polym. Sci.* **1962**, *58*, 1225.
- (22) Saha, P.; Ghosh, P.; Palit, S. R. *J. Polym. Sci.* **1964**, *A2*, 1365.
- (23) Langford, C. H.; Carey, J. H. *Can. J. Chem.* **1975**, *53*, 2431.

corresponding to the counterion of the iron salt used was added in each case. Solutions of iron(III) were prepared in the following way: the required amount of $\text{Fe}(\text{ClO}_4)_3$ was dissolved in deionized water acidified to pH 2.0 with HClO_4 . The ionic strength was regulated to the desired value with NaClO_4 and/or NaCl . For the preparation of ferric chloride complex solutions the iron salts $\text{Fe}(\text{ClO}_4)_3$ with NaCl addition and $\text{FeCl}_3 \cdot 6\text{H}_2\text{O}$ were used. The concentrations of the iron(III) used were usually 0.3–1.0 mM. The iron solutions were freshly prepared each time before use. Measurements with iron solutions can be complicated by the fact that in solutions of iron(II, III) the pH and absorbance change with time.²⁸

Laser Photolysis and Spectrophotometric Observations. Laser photolysis was carried out by using the second harmonic ($\lambda = 347$ nm) of a JK-2000 ruby laser operated in the Q-switched mode. The pulse width was about 15 ns, and the full energy per pulse was ~ 18 mJ. The laser pulse energy was monitored, and the transient traces were normalized during the course of this work. A linear dependence between transient response and the energy of the laser pulse was observed. The mean area of the laser beam was 0.5 cm^2 . The detection of the transient absorption changes was performed via an EGG photomultiplier with a rise time of about 5 ns. The preamplifier full bandwidth at 125 MHz was used to register the signals in the nanosecond range, up to $5 \mu\text{s}$. At longer times the bandwidth was narrowed to 5 MHz. All solutions were used only once to avoid accumulation of the irradiated products. Experiments were performed in 1 cm quartz cells in aerated or deaerated (freeze–pump cycling) solutions at room temperature.

Laser Actinometry. Anthracene was used as an actinometry agent. T–T absorption spectra of the methanolic anthracene solution at controlled laser pulse energy values were measured. Since the intensity distribution of the laser light $I(r)$ in the experiments with iron complexes should be the same as in the experiments with anthracene, it is possible to obtain the value of the product of the quantum yield and molar absorption coefficient of the intermediates from the measurements of the ratio of ΔA_{anthr} to the ΔA values of the intermediates: $\Delta A_{\text{anthr}}/\Delta A = \Phi_{\text{anthr}}^T \epsilon_{\text{anthr}}^T/\Phi\epsilon$. Care was taken during these experiments to have a similar absorbance in the anthracene solution at $\lambda = 347$ nm as in solutions of iron(III). Analysis for the absorbance in solutions was carried out by means of a Hewlett-Packard 8452 diode array spectrophotometer.

Results and Discussion

Photolysis of Ferric Hydroxy Complexes. Figure 1a presents the transient absorption spectrum for an aqueous solution of iron(III) (0.72 mM) at pH 2.90 using $\text{Fe}(\text{ClO}_4)_3$ as starting material. Trace 1 of Figure 1b shows the absorption spectrum of this solution at pH 2.90 and trace 2 at pH 0.5. Figure 1a shows the bleaching band with a maximum at $\lambda = 297$ nm and no transient absorption in the visible region. The latter band corresponds to the absorption maximum of the iron(III) in solution at pH 2.90 as seen in Figure 1b. No meaningful transient signal for these solutions was observed in the UV–visible region at pH < 2 .

The inset in Figure 1a shows the bleaching taking place within the duration of the laser pulse (15 ns). Therefore, whatever transient is formed, it has to be shorter in lifetime than the laser pulse. The coincidence of the maximum positions of the bleaching band (Figure 1a) and absorption band at $\lambda = 297$ nm (Figure 1b) is an indication that the observed bleaching was due to the photolysis of aqueous iron(III) complexes. To ascertain which iron complexes are responsible for the transient absorption, we have to consider the equilibria of the species

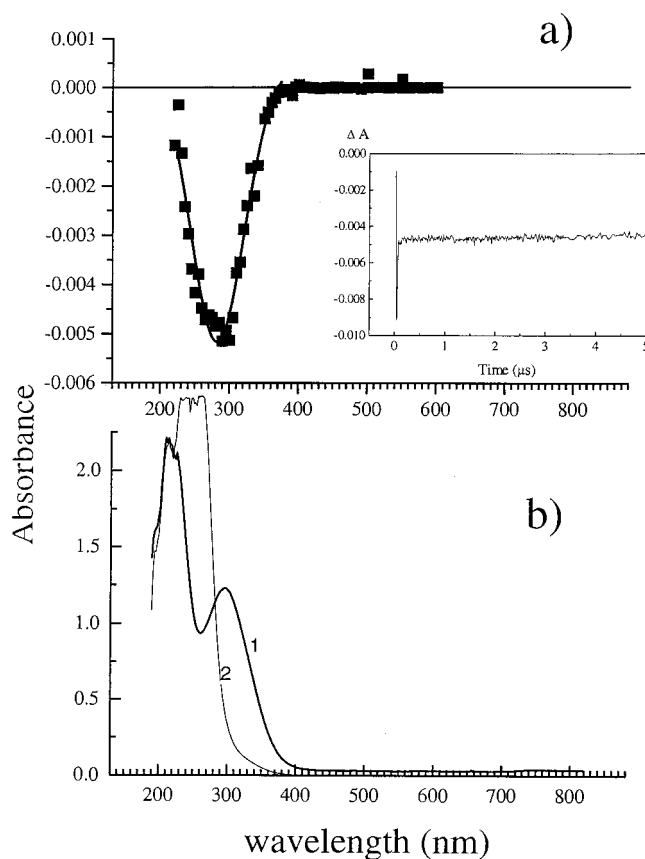
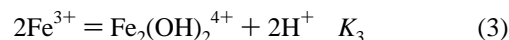
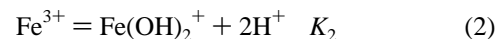


Figure 1. Transient absorption and absorption spectra of the iron(III) aqueous solution ($[\text{Fe}(\text{ClO}_4)_3] = 0.72$ mM without salt addition: (a) transient absorption spectrum (time delay 100 ns at pH 2.90; a transient trace at $\lambda = 300$ nm is shown in the inset); (b) absorption spectra of an iron(III) aqueous solution at (1) pH 2.90 and (2) at pH 0.50.

existing in solution. The hydrolysis of iron(III) in dilute acid solutions has been expressed in eqs 1–3, where the notation of coordination water is omitted.^{3–7}



Equilibrium constants were derived from potentiometric,²³ spectrophotometric,^{3–6,24–26} and kinetic measurements.²⁷ Values for the equilibrium constants are $K_1 = 1.9 \times 10^{-3}$ M and $K_2 = 2.5 \times 10^{-9}$ M² at $T = 25$ °C^{4,5} and $K_3 = 0.8 \times 10^{-3}$ M.⁶ The $\text{Fe}^{3+}_{\text{aq}}$, FeOH^{2+} , $\text{Fe}(\text{OH})_2^+$ and $\text{Fe}_2(\text{OH})_2^{4+}$ ultraviolet spectra, band maxima, and extinction coefficients have been reported in the literature.^{4–6} The concentrations of the different iron(III) complexes and respective absorbances at $\lambda = 347$ nm and $\lambda = 300$ nm have been calculated. They are presented in Table 1. The value of the absorbance at $\lambda = 347$ nm was observed to be 0.47. It is close to the calculated value $\Sigma(A) = 0.478$ (Table 1). The latter value is the summation of the absorbances of the iron species in Table 1. By the same approach the calculated absorbance at $\lambda = 300$ nm had a value of 1.11, whereas the measured absorbance was 1.19. Therefore, a good agreement is found between the experimental and calculated values.

Table 1 indicates that at pH 2.90, the laser light at $\lambda = 347$ nm is absorbed mainly by the FeOH^{2+} complex. The absor-

(24) Olson, A. R.; Simpson, T. R. *J. Chem. Phys.* **1949**, *17*, 1322.

(25) Turner, R. C.; Miles, K. E. *Can. J. Chem.* **1957**, *35*, 1002.

(26) Milburn, R. M.; Vosburgh, W. C. *J. Am. Chem. Soc.* **1955**, *77*, 1352.

(27) Hemmes, P.; Cole, D. L.; Eyring, E. M. *J. Phys. Chem.* **1971**, *79*, 929.

(28) Flynn, C. *Chem. Rev.* **1984**, *84*, 31.

Table 1. Absorption Bands, Extinction Coefficients at $\lambda = 347$ nm and $\lambda = 300$ nm, Concentrations, and Absorbances of Iron(III) Complexes at pH 2.9 and pH 0.5

complex	band max (nm)	$\epsilon_{\lambda=347}$ M ⁻¹ cm ⁻¹	$\epsilon_{\lambda=300}$ M ⁻¹ cm ⁻¹	concn (M)		$A_{\lambda=347}$		$A_{\lambda=300}$
				pH 2.90	pH 0.5	pH 2.90	pH 0.5	pH 2.90
Fe ³⁺ _{aq}	240 ^a	10 ^b	155 ^b	1.72×10^{-4}	7.1×10^{-4}	1.72×10^{-3}	7.1×10^{-3}	2.24×10^{-2}
Fe(OH) ²⁺	205 and 297 ^a	800 ^b	2045 ^b	5.09×10^{-4}	8.4×10^{-6}	0.47	6.9×10^{-3}	1.03
Fe(OH) ₂ ⁺	300 ^a	550 ^b	1291 ^b	8.26×10^{-6}	5.4×10^{-10}	4.5×10^{-3}		1.48×10^{-2}
Fe ₂ (OH) ₂ ⁴⁺	240 and 335 ^b	5000 ^a	1800 ^a	1.5×10^{-5}	4×10^{-9}	1.5×10^{-3}		2.7×10^{-2}
						$\Sigma = 0.478$		$\Sigma = 1.11$

^a pH 0.5. ^b pH 2.9.

bance of the Fe³⁺ aqua-complex is negligible, due to the small molar absorption coefficient of this species at 347 nm.⁴⁻⁶ The absorbances of Fe(OH)₂⁺ and Fe₂(OH)₂⁴⁺ complexes were small relative to that of FeOH²⁺, due to the low concentrations of the first two species in the solution. It is possible to conclude therefore that the observed transient in Figure 1a is due to the excitation of FeOH²⁺. The disappearance of transients at acid pH < 2 follows the shift of the equilibrium in eq 1 from FeOH²⁺ to the Fe³⁺ aqua complex (see Table 1, pH 0.5). This also determines the spectral changes of iron(III) aqueous solutions shown in Figure 1b. Accordingly, the observed transient bleaching can be attributed to the photodissociation



The observed transient bleaching band is explained by the photoreduction of FeOH²⁺ with $\epsilon = 2040 \text{ M}^{-1} \text{ cm}^{-1}$ at $\lambda = 300 \text{ nm}$ ^{4,5} to a ferrous aqua complex having an absorption coefficient below $10 \text{ M}^{-1} \text{ cm}^{-1}$.¹ As a consequence, the observed bleaching band in Figure 1a is a mirror image of the absorbance band of FeOH²⁺ at $\lambda = 297 \text{ nm}$. The quantum yield for FeOH²⁺ dissociation can be obtained by comparing the absorbance of this band with the T-T absorbance of anthracene. The quantum yield is taken here as the fraction of the photodissociated FeOH²⁺ complexes. The ratio of absorbances is $\Delta A(\text{FeOH}^{2+}, \lambda = 300 \text{ nm}) / \Delta A(\text{anthracene}, \lambda = 424 \text{ nm}) = (8.6 \pm 1.7) \times 10^{-3}$. The $\Delta\epsilon_{\text{FeOH}^{2+}}$ value is $\Delta\epsilon_{\text{FeOH}^{2+}} = \epsilon_{\text{Fe}^{2+}} - \epsilon_{\text{FeOH}^{2+}} = -2040 \text{ M}^{-1} \text{ cm}^{-1}$. Using these values and the values of quantum yield of triplet anthracene in alcohol $\phi_T = 0.62$ ³³ and $\Delta\epsilon_{\text{anthr}}(\lambda = 424 \text{ nm}) = 90\,000 \text{ M}^{-1} \text{ cm}^{-1}$,³² the value for the quantum yield of FeOH²⁺ photodissociation is $\phi_{\text{FeOH}^{2+}} = 0.24 \pm 0.06$.

In further experiments phenol (PhOH) was used as the scavenger of OH^{*} radicals formed in reaction 4. Figure 2 shows kinetic curves at $\lambda = 400 \text{ nm}$ for different PhOH concentrations. The inset of Figure 2 shows the absorption spectrum of the iron(III) solution in the presence of PhOH. The split band with a maximum at $\lambda = 400 \text{ nm}$ shows the absorption of the PhO^{*} radical, confirming the OH^{*} formation in reaction 4. These experiments were done at relatively low PhOH concentrations (9×10^{-5} – $4.5 \times 10^{-2} \text{ M}$). This avoided the formation of the complexes between iron(III) and phenol. The rise time of traces in Figure 2 became shorter as the concentration of PhOH increased. The yield of PhO^{*} radical formation was seen to be the same for a variation in the concentration of PhOH by a factor

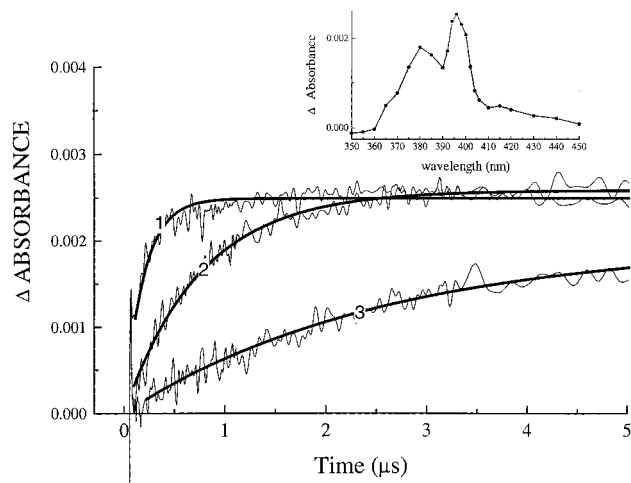


Figure 2. Transients at $\lambda = 400 \text{ nm}$ with $[\text{Fe}(\text{ClO}_4)_3] = 0.70 \text{ mM}$. Photolysis was carried out in the presence of PhOH, pH 2.65. Solid lines are fitting curves corresponding to the rise kinetics $A_{\infty}^*(1 - \exp(-t/\tau))$. (1) $[\text{PhOH}] = 4.5 \times 10^{-2} \text{ M}$. (2) $[\text{PhOH}] = 4.5 \times 10^{-4} \text{ M}$. (3) $[\text{PhOH}] = 0.9 \times 10^{-4} \text{ M}$. The inset shows the transient absorption spectrum at a time delay of 500 ns.

of 100. The kinetics of OH^{*} reaction with PhOH has been studied previously in pulse radiolysis.³⁴ It was shown that the dehydroxybenzene radical was formed as an intermediate, dissociating subsequently with PhO^{*} radical formation. The latter process is not a subject of the present study. From the measurements of the absorbance of PhO^{*} at $\lambda = 400 \text{ nm}$ relative to the T-T absorbance of anthracene at $\lambda = 424 \text{ nm}$, and from the molar absorption coefficient value of PhO^{*} $\epsilon_{\text{PhO}^*} = 2200 \text{ M}^{-1} \text{ cm}^{-1}$,³⁴ a quantum yield of $\phi_{\text{FeOH}^{2+}} = 0.18 \pm 0.03$ was found. This value agrees with the value from the FeOH²⁺ bleaching band observed at $\lambda = 300 \text{ nm}$.

Photolysis of Ferric Chloride Complexes. The equilibria in solution of Fe³⁺ and chloride anions with $K_5 = 5.34 \text{ M}^{-1}$ and $K_6 = 1.82 \text{ M}^{-2}$ are

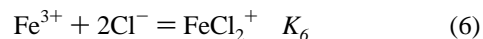
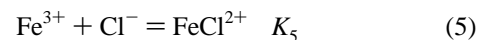


Figure 3 shows the transient spectra for iron(III) species in solution at different delay times after the laser pulse in the presence of Cl⁻ anion ($[\text{NaCl}] = 1 \text{ M}$ and pH 0.6). These spectra agree with the spectra of Cl₂⁻/ClOH⁻ reported in the literature.²⁹ Both Cl₂⁻ and ClOH⁻ species absorb in the range 230–450 nm. In effect, Cl₂⁻ absorption²⁹⁻³¹ has a maximum at $\lambda = 340 \text{ nm}$ with a molar absorption coefficient of $8.8 \times 10^3 \text{ M}^{-1} \text{ cm}^{-1}$. The ClOH⁻ radical²⁹⁻³¹ has a maximum at 350 nm with a molar absorption coefficient of $3.7 \times 10^3 \text{ M}^{-1}$

(29) Jayson, G.; Parson, B.; Swallow, Th. *J. Chem. Soc., Faraday Trans. 1* **1972**, 68, 2053.

(30) Bjergbakke, E.; Navaratnam, S.; Parsons, B. J.; Swallow, A. J. *Radiat. Phys. Chem.* **1987**, 30, 59.

(31) Thornton, A. T.; Laurence, G. S. *J. Chem. Soc., Dalton Trans.* **1973**, 804.

(32) Meyer, Y. H.; Astier, R.; Leclercq, J. M. *J. Chem. Phys.* **1972**, 56, 801.

(33) Murov, S. L.; Carmichael, I.; Hug, G. L. *Handbook of Photochemistry*; Marcel Dekker: New York, 1993.

(34) Land, J.; Ebert, M. *Trans. Faraday Soc.* **1967**, 63, 1181.

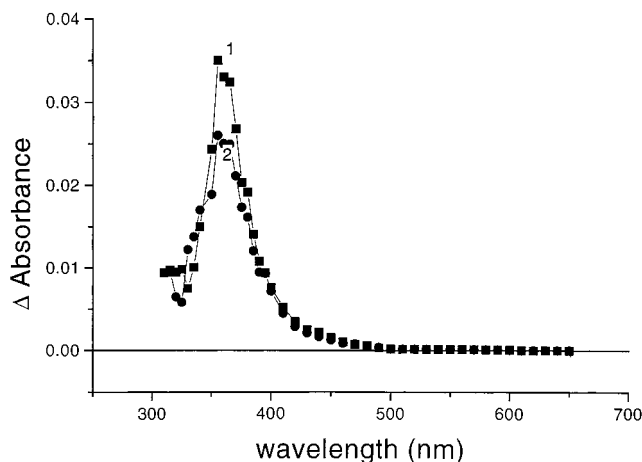


Figure 3. Transient spectra for the laser photolysis of the chloroiron(III) complex (0.7 mM) at pH 0.6 in the presence of NaCl (1 M) salt: (1) time delay 120 ns; (2) time delay 500 ns.

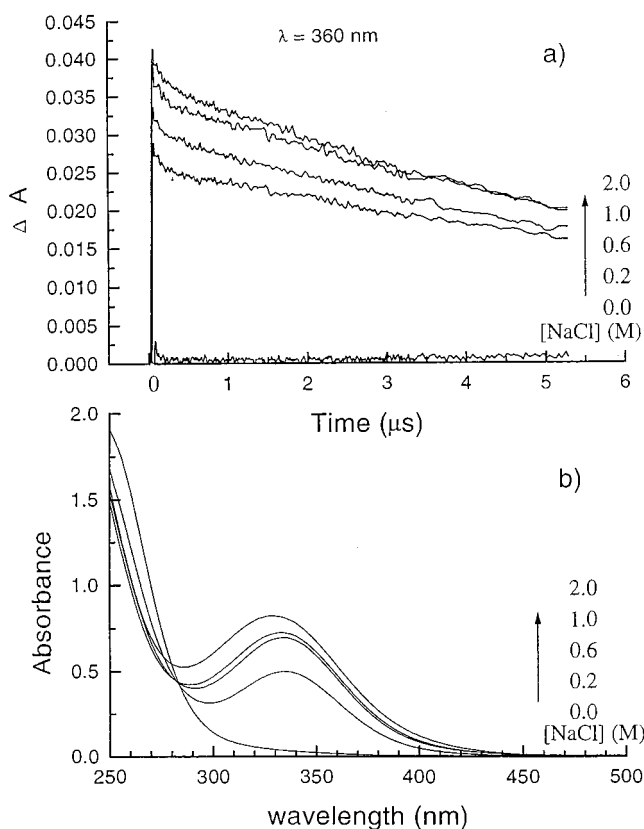


Figure 4. Transients and absorption spectra under iron(III) aqueous solution photolysis in the presence of NaCl ($[\text{Fe}(\text{ClO}_4)_3] = 0.64 \text{ mM}$; ionic strength $s = 2 \text{ M}$): (a) transients at $\lambda_{\text{probe}} = 360 \text{ nm}$ at different NaCl concentrations; (b) absorption spectra of the iron aqueous solution with NaCl added. The concentration of NaCl is indicated.

cm^{-1} . Both species differ mainly in the values of the respective molar absorption coefficients.

Figure 4a shows the transients after the laser pulse using an observation wavelength of $\lambda = 360 \text{ nm}$ for a solution of Fe^{3+} perchlorate in the presence of different concentrations of NaCl (0–2 M) and pH 0.8. The ionic strength was adjusted with NaClO_4 to a value of 2. In Figure 4b the absorption band of the chloroiron complex⁵ at $\lambda = 345 \text{ nm}$ is observed. Its amplitude increases as the Cl^- concentration grows. The transient amplitude in Figure 4a is seen to increase in parallel with ferric chloride added to the solution (Figure 4b). Therefore, it is possible to suggest that chloroiron complexes are the

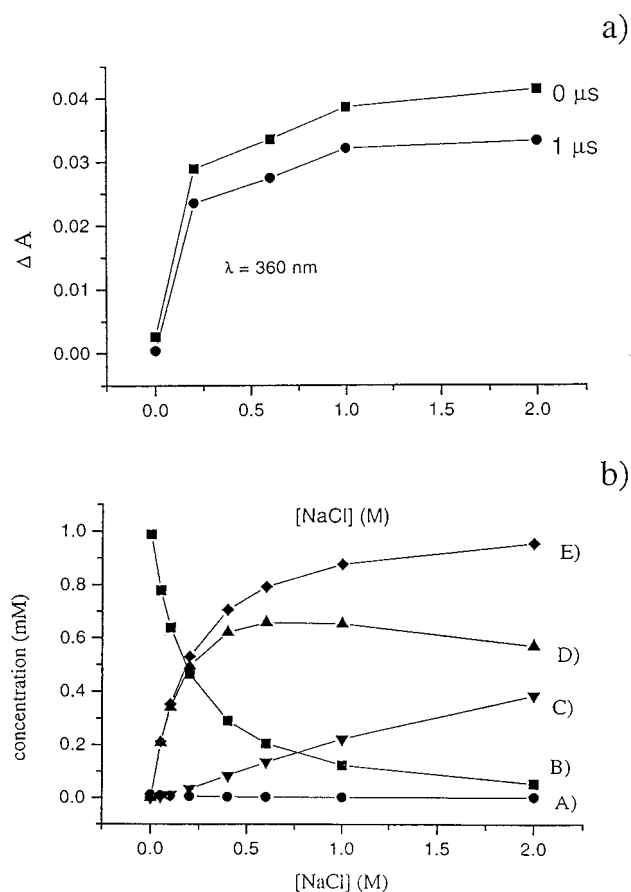


Figure 5. (a) Amplitude of the transient absorption in a solution with $[\text{Fe}(\text{ClO}_4)_3] = 0.64 \text{ mM}$ in a solution of 2 M ionic strength at $\lambda = 360 \text{ nm}$. The NaCl concentrations used are marked. (b) Calculated concentrations of iron(III) complexes in the presence of NaCl at pH 0.8: (A) $[\text{FeOH}^{2+}]$; (B) $[\text{Fe}^{3+}]$; (C) $[\text{FeCl}_2^+]$; (D) $[\text{FeCl}^{2+}]$; (E) $[\text{FeCl}_2^+] + [\text{FeCl}^{2+}]$.

photoactive chromophores giving rise to the transients in Figure 4a. The formation of Cl^\bullet atoms induced by light has been previously reported^{1,2,16–22} as due to FeCl_2^+ and FeCl_2^+ photolysis in the charge-transfer band at 270–400 nm.

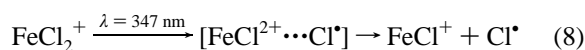
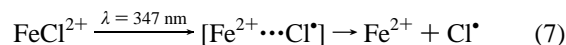
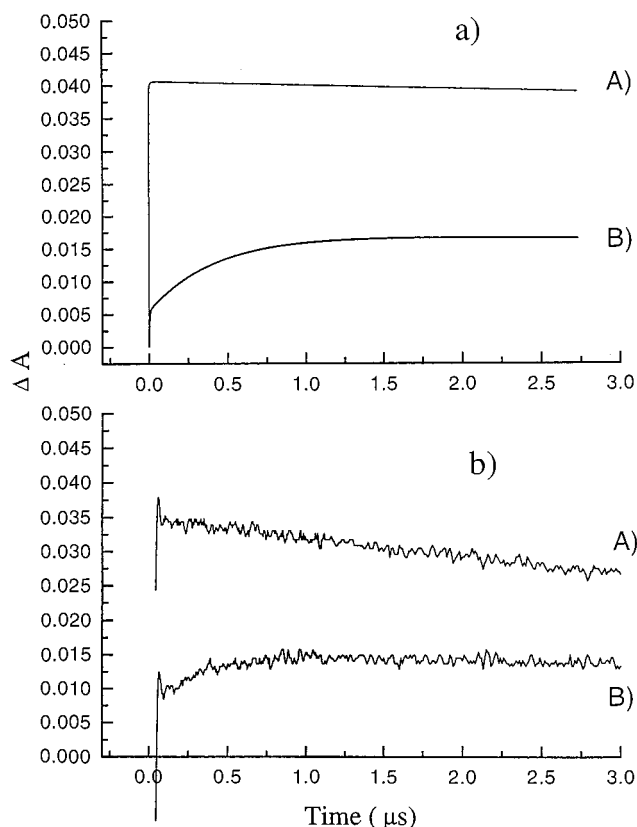


Figure 5a is a continuation of the studies using the same iron complex as in Figure 4 at five different concentrations of NaCl. The amplitude of the transient signals immediately after the laser pulse (0 μs) and at 1 μs is shown in Figure 5a. The variation is seen to be similar in the two cases for the different concentrations of NaCl added in solution. The amplitude of the transient in solution is seen to vary in a similar way at the two times reported in Figure 5a, suggesting only one species in solution.

By way of eqs 1–3, 5, and 6 and the data for the iron(III) equilibrium constants it is possible to obtain the concentrations of the various iron(III) complexes as a function of the NaCl concentration added in solution. Figure 5b shows these results. As seen from Figure 5b, the transients in acid solutions were produced mainly due to FeCl_2^+ and FeCl_2^+ photolysis. The FeOH^{2+} concentration is low (line A in Figure 5b). A parallel

Table 2. The Radical Reactions Involving Cl[•], ClOH[•], Cl₂[•], and OH[•] Radicals

reacn	k ⁺ (forward)	k ⁻ (backward)	ref
Cl [•] + Cl ⁻ = Cl ₂ ^{•-}	2 × 10 ¹⁰ M ⁻¹ s ⁻¹	1.1 × 10 ⁵ s ⁻¹	29
Cl [•] + H ₂ O = ClOH ^{•-} + H ⁺	1.3 × 10 ³ M ⁻¹ s ⁻¹	2.1 × 10 ¹⁰ M ⁻¹ s ⁻¹	29
ClOH ^{•-} = OH [•] + Cl ⁻	6.1 × 10 ⁹ s ⁻¹	4.3 × 10 ⁹ M ⁻¹ s ⁻¹	29
Cl [•] + Fe ²⁺ → Cl ⁻ + Fe ³⁺	5.9 × 10 ⁹ M ⁻¹ s ⁻¹		29
Cl ₂ ^{•-} + Fe ²⁺ → 2Cl ⁻ + Fe ³⁺	1.4 × 10 ⁷ M ⁻¹ s ⁻¹		29
OH [•] + Fe ²⁺ → OH ⁻ + Fe ³⁺	2.3 × 10 ⁸ M ⁻¹ s ⁻¹		29
ClOH ^{•-} + Fe ²⁺ → Cl ⁻ + OH ⁻ + Fe ³⁺			29
Cl ₂ ^{•-} + Cl ₂ ^{•-} → Cl ₃ ^{•-} + Cl ⁻	3.1 × 10 ⁹ M ⁻¹ s ⁻¹		36
Cl ₃ ^{•-} = Cl ₂ + Cl ⁻			
OH [•] + OH [•] → H ₂ O ₂	6 × 10 ⁹ M ⁻¹ s ⁻¹		37

**Figure 6.** Transient kinetics of iron(III) aqueous solutions of iron(III) chloride (0.7 mM) concentration under photolysis at two different pH values. The reported signal has been obtained by following the laser pulse at $\lambda = 370$ nm. (a) Calculated transient kinetics: (A) pH 0.95; (B) pH 1.92. (b) Measured transient kinetics for the same solutions: (A) pH 0.95; (B) pH 1.92.

growth of transient amplitude and FeCl₂²⁺ + FeCl₂⁺ concentration (line E in Figure 5b) was observed for NaCl up to 2 M. However, no parallel growth in the transient amplitude with FeCl₂²⁺ concentration (line D in Figure 5b) was observed at NaCl concentrations higher than 1 M. Below 0.5 M NaCl, the FeCl₂²⁺ concentration (line D in Figure 5) is about 7 times higher than that of FeCl₂⁺ (line C in Figure 5). Therefore, the transient formation at [NaCl] < 0.5 M could be suggested as mainly due to the FeCl₂²⁺ photolysis.

The reactions in Table 2 provide the basis to determine whether Cl₂^{•-} or HClO^{•-} radicals are the main species produced during the chloroiron(III) photolysis. The equilibria between Cl[•], Cl₂^{•-} and OH[•]¹¹ involve reactions in which OH[•] radicals and Cl[•] atoms lead to the formation of Cl₂^{•-}. This has been determined in detail by pulse radiolysis.²⁹⁻³¹

Figure 6a shows the calculated transient curves. Figure 6b presents observed absorption transients at $\lambda = 370$ nm obtained by laser photolysis of iron(III) chloride solutions at pH 0.95

(curve A) and pH 1.92 (curve B). A system of differential equations for the reactions in Table 2 was solved by using the Runge-Kutta algorithm. The system was prepared in a matrix format, inserting the rate and equilibria constants indicated in Table 2. The Runge-Kutta method makes a tentative step for each of the variables (x_1, x_2), which are the points of the interval on which the solution to the differential equations are evaluated by Euler's method. An approximate solution for systems of ordinary differential equations with initial boundary conditions³⁸ is worked out in this way. The function y' is evaluated, and this information is used to adjust the slope (x_1, x_2, \dots). Subsequently the slopes found are adjusted to make a second tentative step and so on.

The expression for the calculated absorbance is $\Delta A(t) = \epsilon_{\text{Cl}_2^{\bullet-}} [\text{Cl}_2^{\bullet-}](t) + \epsilon_{\text{ClOH}^{\bullet-}} [\text{ClOH}^{\bullet-}](t)$, where $[\text{Cl}_2^{\bullet-}](t)$ and $[\text{ClOH}^{\bullet-}](t)$ are the reactant concentrations and $\epsilon_{\text{Cl}_2^{\bullet-}}$ and $\epsilon_{\text{ClOH}^{\bullet-}}$ the respective molar absorption coefficients of 8×10^3 and 3×10^3 M⁻¹ cm⁻¹ at 370 nm.²⁹ The initial concentration of the radicals [Cl[•]] + [OH[•]] was assumed to be 5×10^{-6} M. The concentrations of ferric complexes Fe³⁺, FeOH²⁺, Fe(OH)₂⁺, FeCl²⁺, and Fe(Cl)₂⁺ and of Cl⁻ anions were calculated by the equilibria (1)–(3), (5), and (6) and the corresponding set of algebraic equations. The main feature found in Figure 6 was the slow decay of the absorbance at pH 0.95 and the rising transient observed at pH 1.92. The fair agreement for the calculated and measured transients in parts a and b of Figure 6 suggests that the scheme of the reactions in Table 2 adequately interprets the experimental results obtained. According to these calculations the ClOH^{•-} radical concentration is very low ($\sim 10^{-8}$ M) at both pH 0.95 and pH 1.92.

To estimate the quantum yield of Cl[•] atom formation in eq 7, the ratio of the absorbance of Cl₂^{•-} ($\lambda = 360$ nm) at [NaCl] = 0.5 M to the T-T anthracene absorbance at $\lambda = 424$ nm has been measured. It is $\Delta A(\text{Cl}_2^{\bullet-}, \lambda = 360 \text{ nm}) / \Delta A(\text{anthracene}, \lambda = 424 \text{ nm}) = (5.7 \pm 1.3) \times 10^{-2}$. This value is used to estimate the quantum yield of Cl[•] atom formation in reaction 7. Due to the lower FeCl₂⁺ concentration relative to that of FeCl₂²⁺ at [NaCl] = 0.5 M, reaction 8 can be neglected in relation to Cl[•] formation. All Cl[•] atoms would be scavenged by Cl⁻ anions in the reaction leading to Cl₂^{•-} radical formation, as shown by the reaction on the top in Table 2. As seen from reactions 7 and 9, the concentration of Cl₂^{•-} coincides with the concentration of photodissociated FeCl₂²⁺. Since ferrous complexes do not absorb at $\lambda = 360$ nm, then at this λ the value of $\Delta A = \epsilon_{360\text{Cl}_2^{\bullet-}} [\text{Cl}_2^{\bullet-}] - \epsilon_{360\text{FeCl}_2^+} [\text{FeCl}_2^+]_{\text{dissociated}}$ is much larger than $\Delta A = \Delta \epsilon^{360} [\text{FeCl}_2^+]_{\text{dissociated}}$. The differential absorption coefficient at 360 nm is given by $\Delta \epsilon = \epsilon_1 - \epsilon_2 = 6400$ M⁻¹

(35) Adamson, M. G.; Baulch, D. L.; Dainton, F. S. *Trans. Faraday Soc.* **1962**, *58*, 1388.

(36) Elliot, A. *Radiat. Phys. Chem.* **1989**, *34*, 753.

(37) Sichev, A.; Isak, V. *Usp. Khim.* **1995**, *64*, 1183 (Russian edition).

(38) The program used is described in: Byrne, G.; Hindmarsh, A. *ACM Trans. Math. Software.* **1975**, *1*, 71–96.

cm^{-1} , where ϵ_1 and ϵ_2 are the extinction coefficients of $\text{Cl}_2^{\bullet-}$ and FeCl^{2+} with values of 8000 and $1600 \text{ M}^{-1} \text{ cm}^{-1}$, respectively. The quantum yield for the photodissociation of FeCl^{2+} was found to be 0.46 ± 0.11 .

As with the FeOH^{2+} complex, PhOH can be used as a scavenger for Cl^\bullet atoms or $\text{Cl}_2^{\bullet-}$ radicals during photolysis of FeCl^{2+} for the estimation of the quantum yield of primary photodissociation. A transient spectrum for the PhO^\bullet radical with a characteristic split absorption band at $\lambda = 400 \text{ nm}$ was observed during the photolysis of Fe^{3+} perchlorate in the presence of $[\text{NaCl}] = 0.5 \text{ M}$ and $[\text{PhOH}] = 0.05 \text{ M}$ at pH 0.8. The ratio of the absorbance at 400 nm of the PhO^\bullet radical to that of the T–T transition in anthracene was found to be 0.022 ± 0.005 . From these data the quantum yield of FeCl^{2+} photodissociation has been estimated to be 0.57 ± 0.13 . It is in agreement with the value reported above from the $\text{Cl}_2^{\bullet-}$ radical yield measurements.

The formation of $[\text{Fe}^{2+\cdots\text{X}^\bullet}]$ pair ($\text{X} = \text{HO}^\bullet, \text{Cl}^\bullet$) in reactions 4 and 7 and the primary geminate recombination reaction (cage effect) have been discussed.¹ The existence of long-lived excited states $[\text{FeX}^{2+}]^*$ has also been suggested.¹ The inset in Figure 1a showing the FeOH^{2+} bleaching indicates that no excited $[\text{FeOH}^{2+}]^*$ state is formed with a lifetime longer than the laser pulse duration. No indications of the relaxation processes can be obtained from the observed trace $> 50 \text{ ns}$. On the other hand, the lifetime of the pair $[\text{Fe}^{2+\cdots\text{OH}^\bullet}]$ should also be below 50 ns because no relaxation trace above 50 ns in the inset was observed in Figure 1a. The kinetics of $\text{Cl}_2^{\bullet-}$ radical formation shown in Figures 4a and 6 shows that the dissociation of FeCl^{2+} complex takes place below 50 ns. The traces observed for $\text{Cl}_2^{\bullet-}$ at time delays longer than 50 ns can be accounted for without involving the $[\text{FeCl}^{2+}]^*$ or $[\text{Fe}^{2+}\text{Cl}^\bullet]$ species. Considering $[\text{Fe}^{2+\cdots\text{X}^\bullet}]$ dissociation as diffusion radical escape from the cage, the lifetime of the pair is less than 1 ns in accordance with Eigen's equation.³⁹ Fe^{2+} and Fe^{3+} ions are labile species with ligand substitution rates of ca. $10^6 \text{ M}^{-1} \text{ s}^{-1}$ for $\text{Fe}^{2+}_{\text{aq}}$ and ca. $10\text{--}10^2 \text{ M}^{-1} \text{ s}^{-1}$ for $\text{Fe}^{3+}_{\text{aq}}$.³¹ The water exchange rate for the ion $\text{Fe}^{2+}_{\text{aq}}$ is $3.2 \times 10^6 \text{ s}^{-1}$.³¹ Considering the dissociation of $[\text{Fe}^{2+\cdots\text{X}^\bullet}]$ as a ligand substitution reaction, the lifetime of the complex can be expected in the range of 20–300 ns. The ligand substitution in $[\text{Fe}^{2+\cdots\text{X}^\bullet}]$ can be compared with the time resolution in the present experiments. The mechanism of photodissociation of FeX^{2+} can therefore be considered as a ligand substitution reaction accompanied by electron transfer.

Comparison of Quantum Yield of FeOH^{2+} and FeCl^{2+} Photodissociation Determined from the Laser and Steady-State Photolysis. From steady-state experiments it is known that the quantum yield for Fe^{2+} formation due to FeOH^{2+} photolysis is low in the absence of scavengers ($\phi \approx 10^{-4}$), since a primary process producing Fe^{2+} and hydroxyl radicals would be subjected to thermal reversal. To determine the primary

quantum yield of Fe^{3+} photoreduction to Fe^{2+} species, various workers have explored iron isotope exchanges between the two oxidation states,³⁵ radical-initiated polymerizations,¹⁶ alcohol scavenging,^{10,23} and reduction of iron(III) in solution at low iron(III) concentration.⁷ The quantum yield of the FeOH^{2+} dissociation was reported to be 0.14 ± 0.04 at for the photolysis at $\lambda = 313 \text{ nm}$; 0.017 ± 0.003 at $\lambda = 360 \text{ nm}$ (ionic strength 0.03),⁷ and between 0.14 and 0.19 at $\lambda = 313 \text{ nm}$.¹ The quantum yield $\phi_{\text{FeOH}^{2+}}$ obtained in this study lies between 0.18 and 0.24 at $\lambda = 347 \text{ nm}$. It is about 50% higher than for the photodissociation of the FeOH^{2+} complex reported by steady-state measurements at 313 nm.^{1,7} Also, the photodissociation quantum yield at $\lambda = 347 \text{ nm}$ observed in this study was higher than the quantum yield obtained by steady-state photolysis at $\lambda = 360 \text{ nm}$. The difference between the quantum yields for photolysis at $\lambda = 313 \text{ nm}$ and $\lambda = 360 \text{ nm}$ in steady-state experiments can be due to the effect of the light photon energy. The probability of the photodissociation of FeOH^{2+} may be a function of the excess energy made available to the $[\text{Fe}^{2+\cdots\text{OH}^\bullet}]$ pair dissociation.¹ The quantum yield value from the laser photolysis experiments at $\lambda = 347 \text{ nm}$ relative to steady-state measurements at $\lambda = 313 \text{ nm}$ and $\lambda = 360 \text{ nm}$ is in agreement with the suggestion of the effect of the light photon energy.

By photopolymerization studies a quantum yield of dissociation of FeCl^{2+} of 0.13 has been reported in the range 300–400 nm.^{1,17} A modest quantum yield of Cl^\bullet atom formation^{19,20} has been reported by photopolymerization along with a quantum yield of 0.093 by steady-state photolysis at $\lambda = 350 \text{ nm}$ ²³ using *tert*-butyl alcohol as scavenger. The present measurements found a value of 0.46–0.57 for the quantum yield of photodissociation of FeCl^{2+} . This is about 5 times higher than from the steady-state measurements in aqueous solution. During steady-state photolysis the initial generation step of the radicals and the termination step of the reaction are both important, whereas only the former would have a determining influence during the generation of radicals in solution by pulsed laser photolysis. The $\text{Cl}_2^{\bullet-}$, Cl^\bullet , and Cl_2 (from $\text{Cl}_2^{\bullet-}$ decay) can reoxidize the ferrous photochemical products in a steady-state situation. However, in the pulsed laser case these reactions in solutions are too slow to be effective.

Note that the quantum yield of photodissociation of FeCl^{2+} observed in the present work is about twice the value found for FeOH^{2+} . The OH^\bullet radical is known to be a stronger oxidizer than the Cl^\bullet atom, making the excess energy available ($\sim 0.1 \text{ eV}$) for FeCl^{2+} photodissociation higher than the energy available for the photodissociation of FeOH^{2+} . This could be a further indication of the effect of the absorbed light energy on the quantum yield of FeX^{2+} photodissociation.

Acknowledgment. This work was supported by the European Community Environmental Program ENV-CT 95-0064 (OFES No. 96.350, Bern, Switzerland).

(39) Eigen, M. Z. *Phys. Chem.* **1954**, 89, 1095.